DAΦNE TECHNICAL NOTE

INFN - LNF, Accelerator Division

Frascati, September 20, 1994

Note: **G-27**

OPTICAL CHARACTERISTICS OF THE DAΦNE WIGGLER

M. Bassetti, C. Biscari, M.A. Preger

ABSTRACT

The prototype of the DAΦNE wiggler, built by DANFYSIK, has been delivered to LNF in January 94. Measurements of the magnetic field have been carried out[1]. From the analysis of these measurements the nominal beam trajectory inside the wiggler has been calculated and the multipolar expansion of the field has been deduced.

1. INTRODUCTION

Wigglers have been included in the DAΦNE lattice to increase damping and tune the emittance for luminosity optimization. Four of them are placed inside the achromats, where the dispersion is high (see Fig. 1). Their field modifies the synchrotron integrals I_2, I_3, and I_5[2], thus changing the emittance and the natural energy spread of the beams. Taking into account only linear terms in its field expansion, a wiggler acts as a drift in the horizontal plane, while in the vertical one it is equivalent to a distributed quadrupole. The vertical beam size is kept small and almost constant along the wiggler by forcing the betatron function to coincide with the self-beta of the equivalent quadrupole. At the second order the wiggler has real sextupolar terms and pseudo sextupolar terms[3].

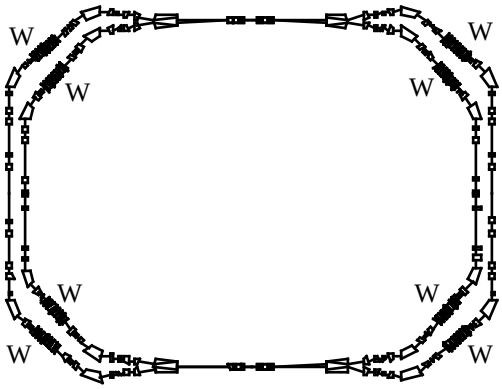

Fig. 1 - DAΦNE main rings layout

The DAΦNE wiggler is composed by 5 full poles plus two half poles at the ends, with a maximum field of 1.8 T and a total length of 2 m. Two power supplies per wiggler are used, the first for the 5 central poles, the second for the two end poles, so that adjustments to the field integral can be made by changing the end pole field.

The field model used up to now for lattice calculation purposes, shown in Fig. 2, represents each pole by a central parallel face bending magnet, with a half field rectangular magnet on each side, which accounts for the fringing fields. The nominal central trajectory, given in Fig. 3, lies on one side of the machine axis, with a maximum displacement with respect to this axis of 2.469 cm.

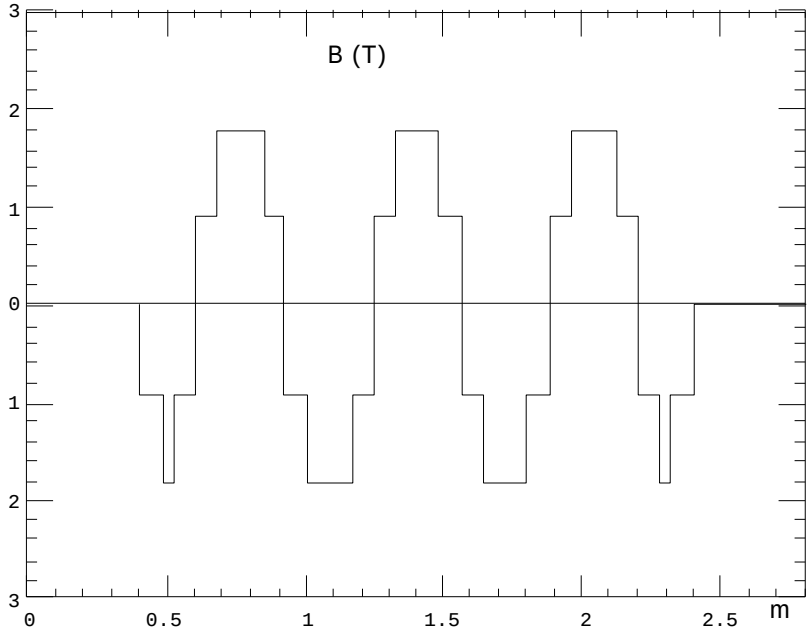

Fig. 2 - Wiggler field model

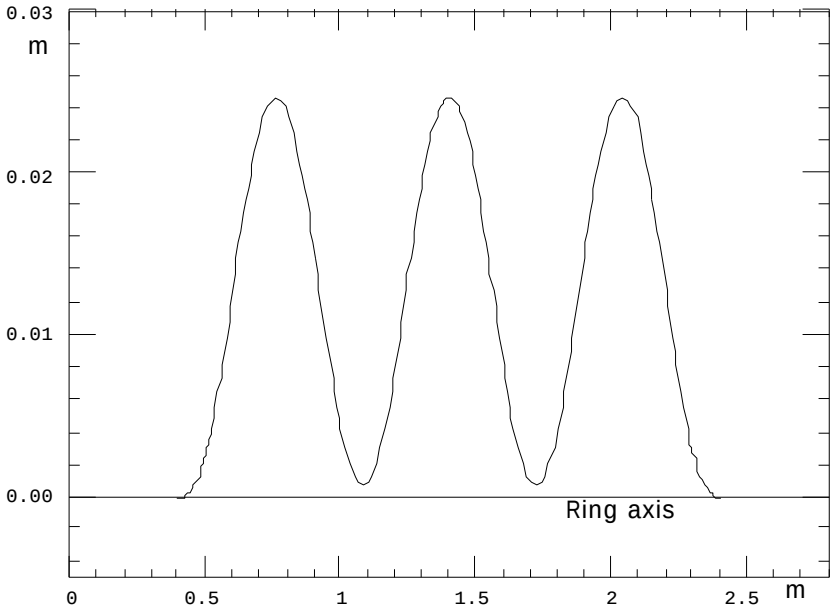

Fig. 3 - Beam central trajectory corresponding to the field model

The analysis of field measurements allowed to check the reliability of this model and to investigate the effects of the wiggler on the storage ring optics.

2. MAGNETIC MEASUREMENTS ANALYSIS

The complete description of the mechanical and electrical parameters of the wiggler is given in [1], together with the results of magnetic measurements.
In our coordinate system x, y, and z correspond to the horizontal, vertical and longitudinal directions respectively.

The field is measured by longitudinal scans of the vertical field component at fixed horizontal and vertical positions. Each scan delivers therefore a table containing the value of the vertical component of the magnetic field, B_y, for constant x and y, along the z direction, in steps of 2 cm, for a total number of 140 points, extending 40 cm before and after the mechanical length of the device. Scans at different values of x have been performed, both on the symmetry plane of the wiggler, corresponding to y = 0, and on the two planes y = ± 5 mm. For y = 0 and y = -5 mm it is possible to scan the horizontal position of the probe from -2 cm to +3 cm from the wiggler axis in 5 mm steps. For y = 5 mm, the horizontal range is from -3 cm to + 3 cm. As it will be described in the following, this system is not optimized for our purposes, where neighbouring points in x and y are compared to find out high order derivatives. We strongly suggest to repeat the measurements with the three dimensional coordinatometer now available in the magnetic measurements laboratory.

Among all the performed measurements[1], those used for our field analysis are summarized in Table I.

Table I - Summary of analyzed data

SCAN	Date	I Central Poles (A)	I End Poles (A)	X (cm)	Y (cm)	∫Bdl (g m)
1	21.3.94	712.8	562.1	-2	0.0	-1.5
2	21.3.94	712.8	562.1	-1	0.0	3.5
3	21.3.94	712.8	562.1	0	0.0	5.4
4	21.3.94	712.8	562.1	1	0.0	2.4
5	21.3.94	712.8	562.1	2	0.0	-1.0
6	21.3.94	712.8	562.1	3	0.0	-4.4
7	23.3.94	712.8	562.1	0	-0.5	8.8
8	23.3.94	712.8	562.1	0	0	6.7
9	23.3.94	712.8	562.1	0	0.5	6.6

A sketch of the grid in the (x,z) plane is shown in Fig. 4. From the value of the field on the grid nodes we extrapolate the field inside each case. An example of the field behaviour (corresponding to scan n.3) along z is given in Fig. 5, while an example of the behaviour along x at the pole center (taken from scans 1 to 6) is shown in Fig. 6. It is reasonable to use a different kind of interpolation for the two directions.

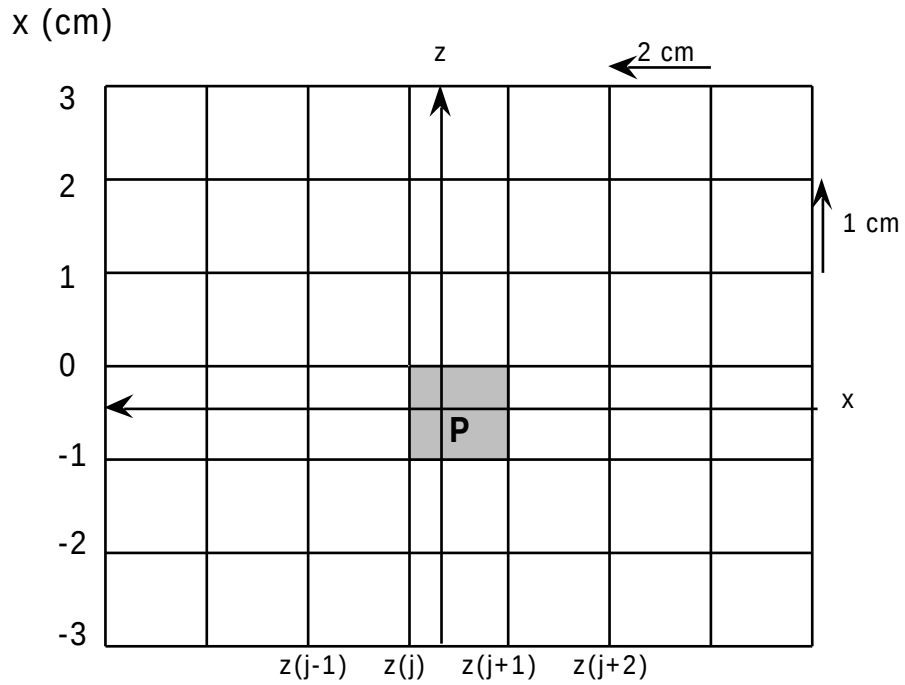

Fig. 4 - Data grid in the plane (x,z)

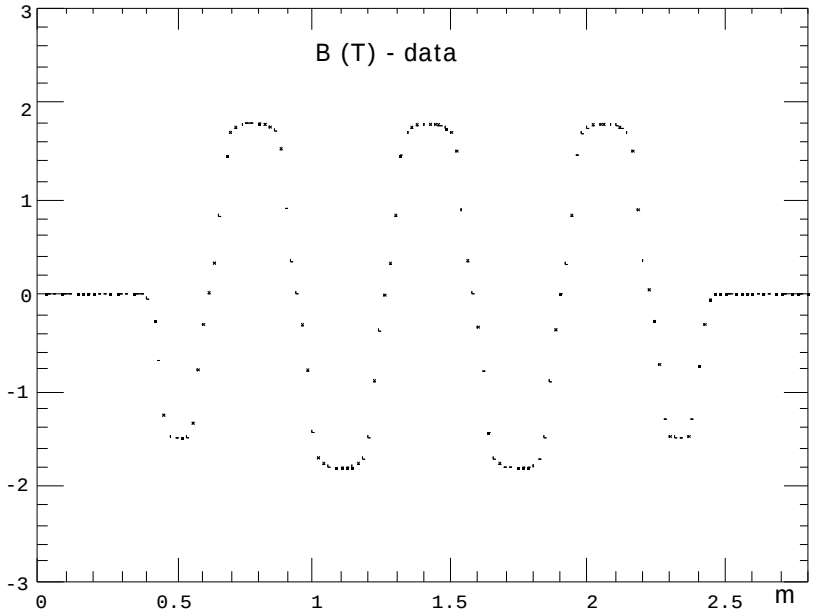

Fig. 5 - Measured B_y along z (data n.3)

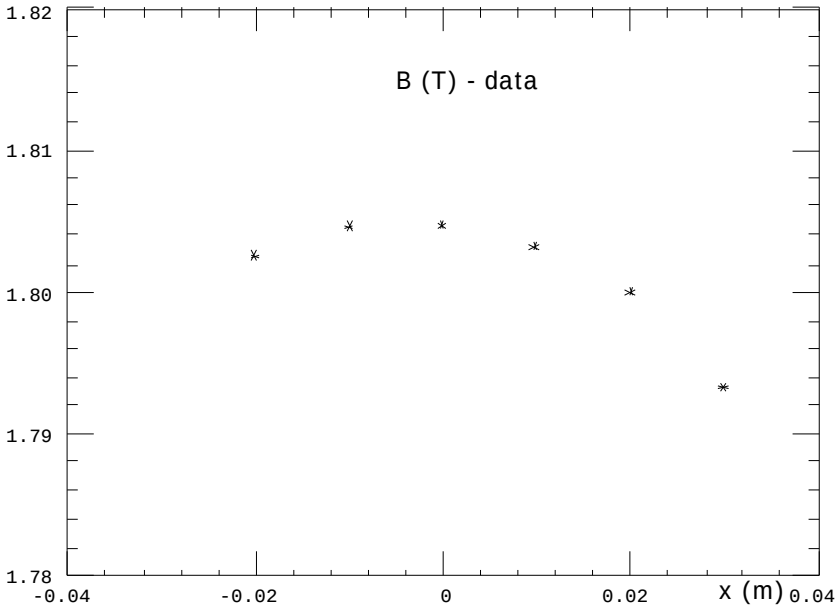

Fig. 6 - Measured B_y along x (data n.1/6)

Polynomial interpolation along z

The function $B_y(x_i,y_k,z)$ for each longitudinal segment of the grid (see Fig. 4) is represented as a 3rd order polynomial

$$B_y(x_i,y_k,z) = \sum_{j=1}^{4} A_{ij}\, z^{\,j-1}$$

The coefficients are computed from the two edge points of the segment plus the two adjacent ones, by a polynomial interpolation, using the NAG library routine E01AEF[4] .

The interpolated function, together with the measured values (scan n. 3), are plotted in Fig. 7.

Figure 8 shows a zoom of the same plot, to check the continuity of the function in the grid points.

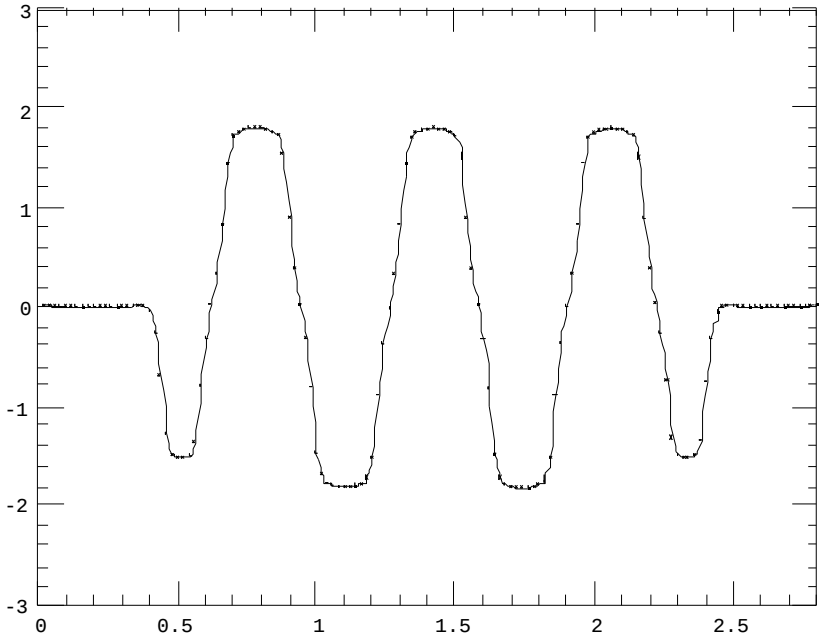

Fig. 7 - Interpolated function $B_y(0,0,z)$ together with the data

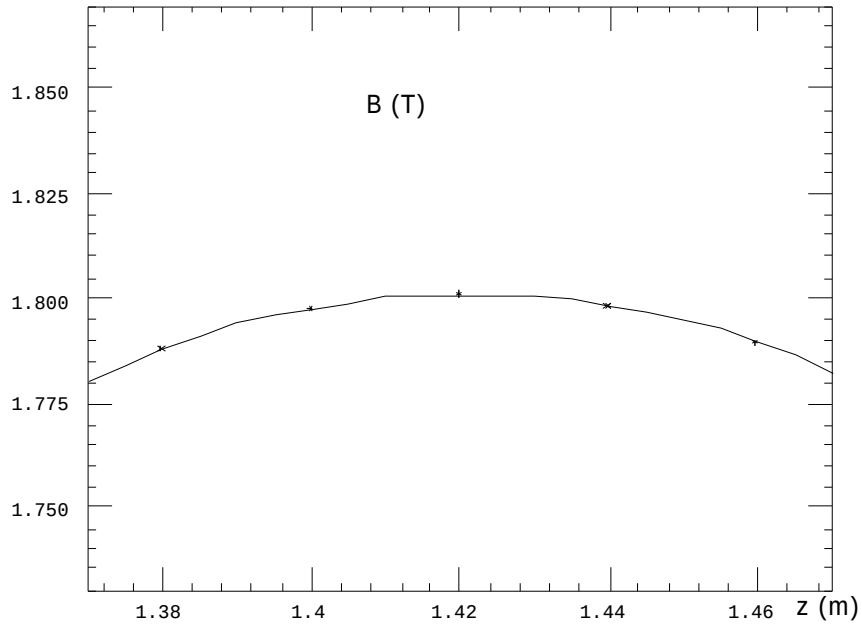

Fig. 8 - Zoom of $B_y(0,0,z)$ from Fig. 7

As explained in [1] successive measurement at different x can be performed only after completely extracting the carriage from its guiding box outside the wiggler; the initial carriage positioning accuracy is of the order of 0.1 mm. To correct the longitudinal shifts of the data from different scans, we have applied a realignment procedure: all the points of each scan have been shifted on the interpolated function by a quantity $<\Delta z>$, which is the average shift of the four central zeros of the function $B_y(x_i,y_k,z)$ with respect to the zeros of the function $B_y(0,y_k,z)$ Table II gives the values of $<\Delta z_i>$; the table shows also the values of a second shift $<\Delta z'_i>$,where the difference is taken with respect to $B_y(0,0,z)$. Of course, being y=0 in the first 6 scans (see Table I), $<\Delta z_i>$ and $<\Delta z'_i>$ are the same. After correction the values of the single zeros of the interpolated functions coincide with the reference scan at x=0 within ≈10 μ, demonstrating that the assumption of a shift in the initial position is correct.

TABLE II - Relative shifts of different scans

SCAN	DATE	$<\Delta z_i>$ (m)	$<\Delta z'_i>$ (m)
1	21.3.94	$-9.08\ 10^{-5}$	$-9.08\ 10^{-5}$
2	21.3.94	$6.01\ 10^{-5}$	$6.01\ 10^{-5}$
3	21.3.94	0.	0.
4	21.3.94	$1.47\ 10^{-4}$	$1.47\ 10^{-4}$
5	21.3.94	$-6.26\ 10^{-5}$	$-6.26\ 10^{-5}$
6	21.3.94	$1.46\ 10^{-4}$	$1.46\ 10^{-4}$
7	23.3.94	$-2.73\ 10^{-4}$	$6.08\ 10^{-4}$
8	23.3.94	0	$3.35\ 10^{-4}$
9	23.3.94	$4.95\ 10^{-5}$	$3.85\ 10^{-4}$

Parabolic fitting along x

From the functions $B_y(x_i,0,z)$ we can now obtain $B_y(x,0,z)$ as:

$$B_y(x,0,z) = \sum_{j=0}^{2} a_j(z)\, x^j$$

where the coefficients $a_j(z)$ are fitted over the values of $B_y(x_i,0,z)$ for $1 \le i \le 6$.

Parabolic interpolation along y

The variation of B_y along y has been derived from scans 7÷9, measured on the same day. Having only three points for each value of z, a parabolic interpolation has been performed.

$$B_y(0,y,z) = \sum_{j=0}^{2} b_j(z)\, y^j$$

3. TRANSVERSE FIELD COMPONENT ALONG Z

Expressing $B_y(x,0,z)$ as the quadratic function:

$$B_y(x,0,z) = a_o(z) + a_1(z)\, x + a_2(z)\, x^2$$

the three coefficients $a_o(z)$, $a_1(z)$, $a_2(z)$ are shown in Figs. 9 for scans 1÷6, while the vertical behaviour corresponding to x=0 is:

$$B_y(0,y,z) = b_o(z) + b_1(z)\, y + b_2(z)\, y^2$$

and coefficients $b_1(z)$, $b_2(z)$ are represented in Figs. 10 for scans 7/9. ($b_o(z) = a_o(z)$).

The second derivative $\partial^2 B_y(0,0,z)/\partial z^2$ with respect to z is plotted in Fig. 11 for scan n. 3.

The dipolar $a_o(z)$ term represents of course the field behaviour on the wiggler axis. The $a_2(z)$ and $b_2(z)$ terms, proportional to the second derivatives of the field with respect to x and y, and the second derivative with respect to z will be used to compute the multipolar expansion of the field. The horizontal quadrupolar term $a_1(z)$ is very weak, and its presence can be explained as a right-left asymmetry with respect to the longitudinal axis of the structure. The vertical quadrupole term $b_1(z)$ has not been explained; it may come, in principle, from an asymmetry between the two vertical positionings of the probe, within the experimental errors, producing a linear component of the field proportional to the quadratic term.

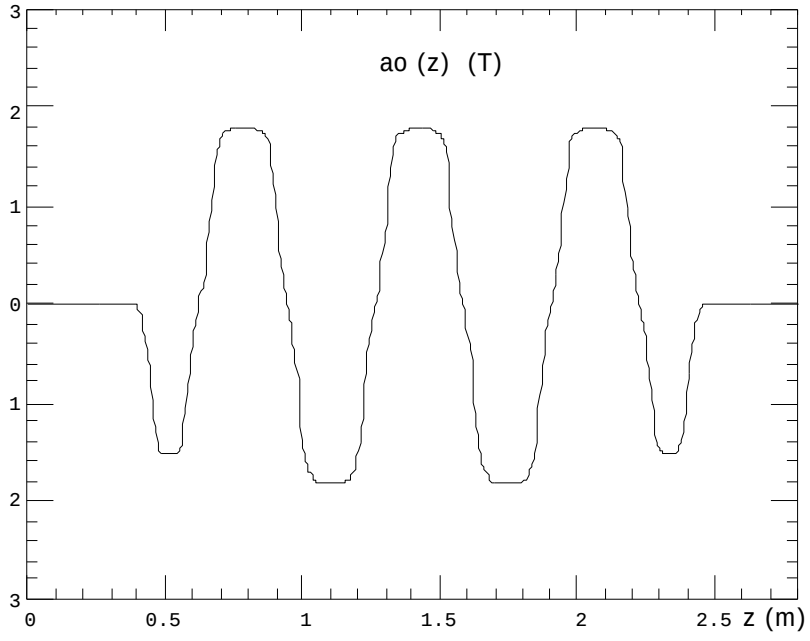

Fig. 9a - Function $a_o(z)$

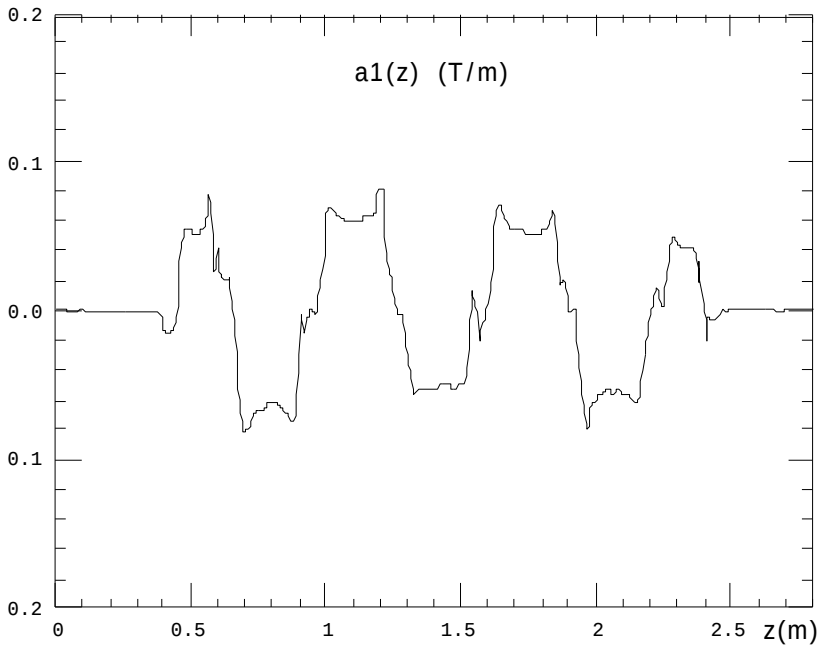

Fig. 9b - Function $a_1(z)$

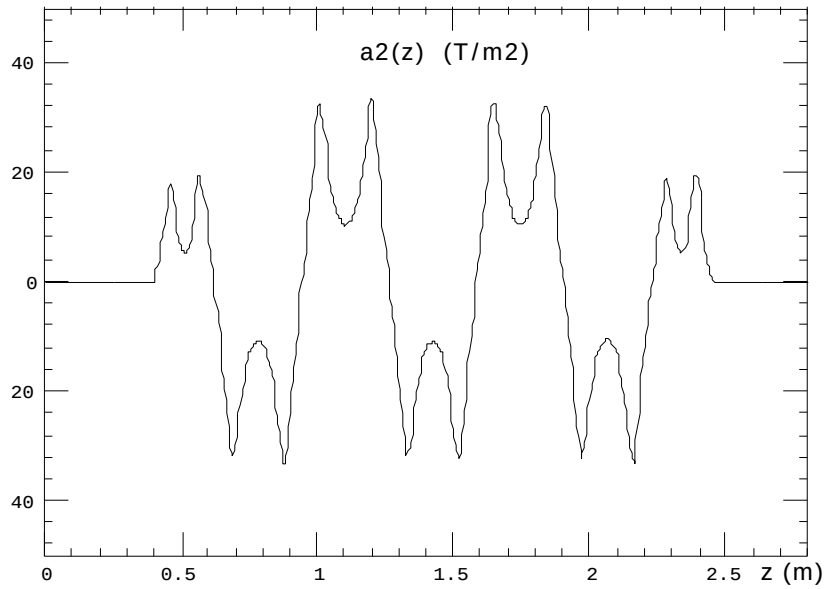

Fig. 9c - Function $a_2(z)$

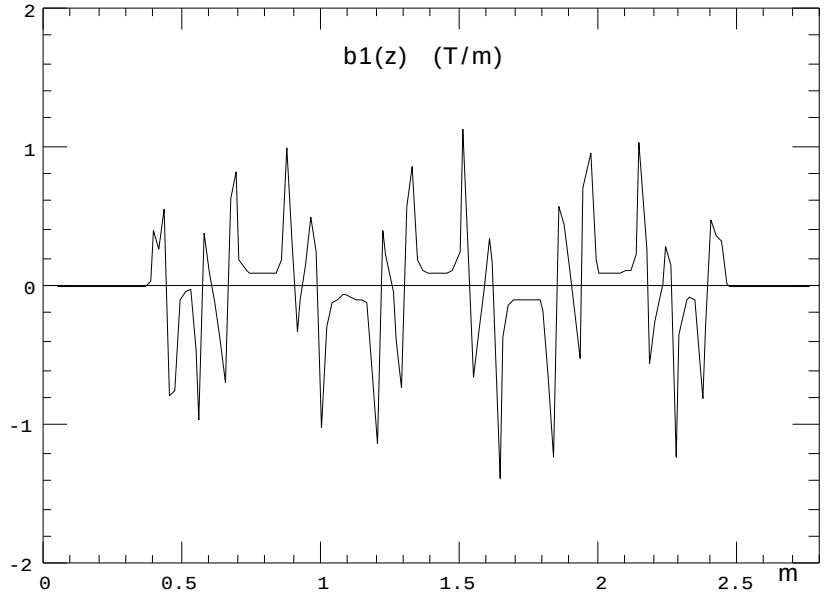

Fig. 10a - Function $b_1(z)$

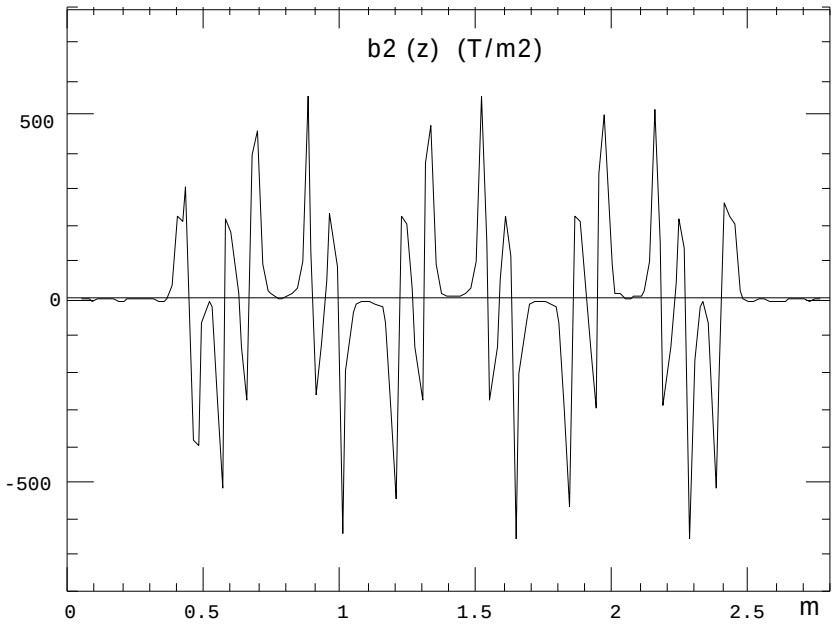

Fig. 10b - Function $b_2(z)$

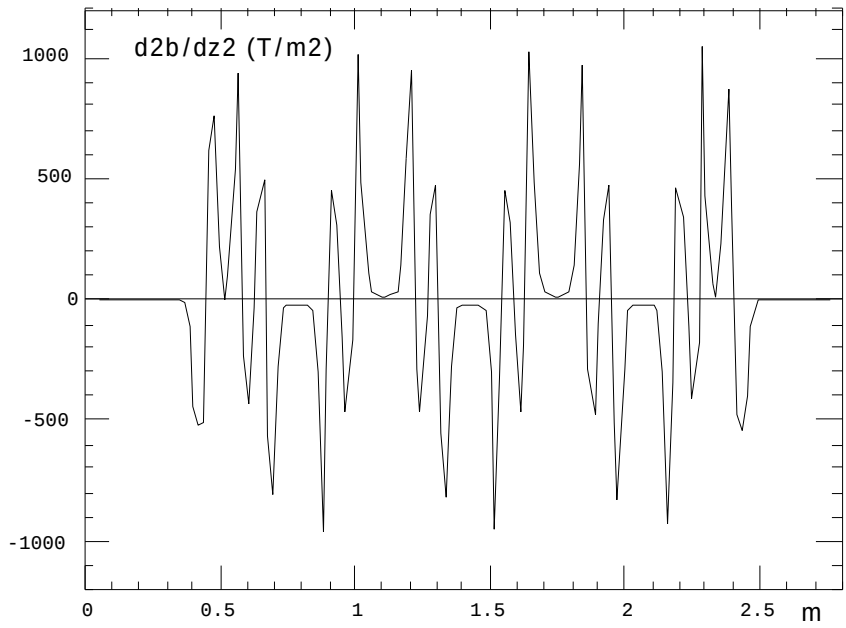

Fig. 11 - $\frac{\partial^2 B_y}{\partial z^2}$ *for scan n. 3*

4. BEAM CENTRAL TRAJECTORY

Let 's assume that the wiggler has a mechanical symmetry with respect to the y = 0 and x = 0 planes and to the center of the z axis (z = 0); in this case the field $B_y(x,0,z)$ coincides with the total field. A trajectory with initial conditions y = 0, y' = 0 remains in the y = 0 plane for any initial conditions x_{in}, and x_{in}'. From the beam dynamics point of view the trajectories at the nominal energy which satisfy the conditions:

$$x_{fin} = x_{in},$$

$$x'_{fin} = x'_{in} = 0$$

are particularly important. Each of them can be a "beam central trajectory" if the wiggler axis is displaced from the ideal ring orbit by x_{in}. Denoting by z_F and z_C the coordinates of the end and central points of the wiggler, the field integral along these trajectories must vanish, namely:

$$\int_0^{s(z_F)} B_y \, ds = 0.0$$

and due to the symmetry assumptions also:

$$\int_0^{s(z_C)} B_y \, ds = 0.0$$

It is clear that for given main pole and end pole currents the previous conditions are satisfied only for a particular x_{in}.

Figure 12 shows the value of the field integral along the trajectory as function of x_{in} for the main and end pole currents in Table I.

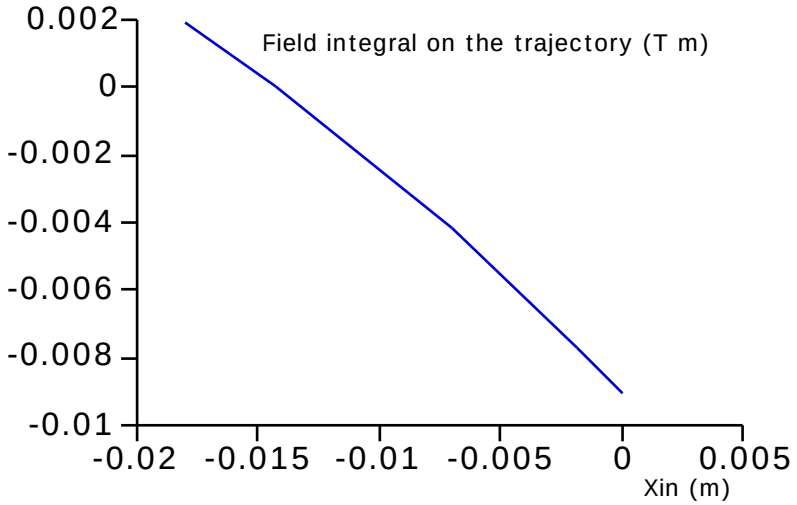

Fig. 12 - Field integral along the trajectory as function of initial coordinate

In this case the right x_{in} should be ≈ -1.5 cm. It is clear that modifying the end pole currents we can satisfy the previous conditions for a large range of different x_{in}.

Figure 13 shows the integral field measured on the wiggler axis (not on the trajectory), giving a good approximation to variation of the integral on the trajectory as a function of the end poles current.

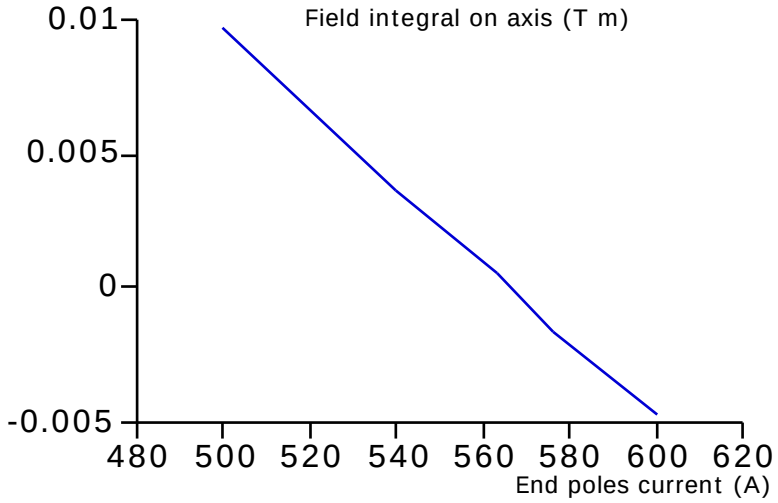

Fig. 13 - Field integral on axis as a function of end poles current

Therefore in principle we could choose any x_{in}. However, we can base the choice of x_{in} on the following physical considerations.

When the field integral is zero on the axis, and the initial trajectory coordinates are (0.,0.) the trajectory is not compensated. In fact the trajectory spends almost the same time where the field is negative and where it is positive; entering on the axis, it passes through the negative field where this one is at its maximum absolute value, while through the positive one it is displaced by ≈2.5 cm from the axis, where the field is lower because of its quadratic behaviour (see Fig. 6); the field integral on the trajectory is therefore negative (of the order of 0.01 T m). But this is not the main drawback of this choice for the initial conditions. As explained before, by varying the end poles current it should be possible to get also in this case a central beam trajectory. The main problem of this choice is that the trajectory lies all on a single side with respect to the wiggler axis, and therefore it does not exploit 50% of the good field region. The best choice, from this point of view, is to displace the wiggler axis with respect to the ideal beam trajectory in the straight section by half the amplitude of the trajectory in the wiggler: according to the data, for 712.8 A in the central poles, yielding a maximum field of 1.8 T, and 562.1 A on the end poles, corresponding to almost vanishing field integral, the wiggler axis must be displaced with respect to the ring axis by 1.45 cm.

For the set of data 1÷6 in Table I the central beam trajectory has been computed. Fig. 14 shows the trajectory starting on axis, and the one entering with x_{in}=-1.451 cm; the latter comes out with an angle negligible with respect to the measurement error in the field integral and x_{out}=-1.471 cm; The 0.2 mm difference between x_{in} and x_{out} is due to a small asymmetry of the wiggler field with respect to its center; its value is within the alignment tolerances of the ring, and hence manageable with the orbit correction scheme.

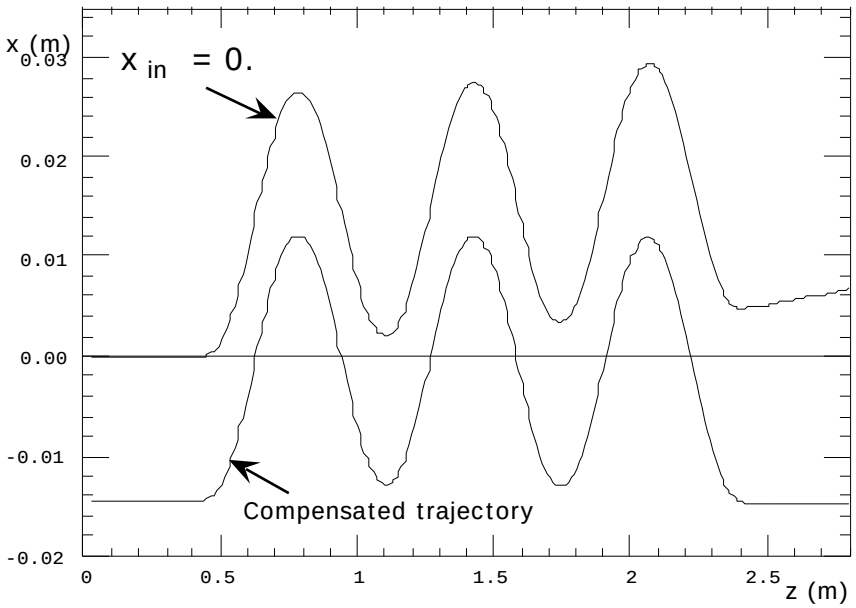

Fig. 14 - Beam central trajectories: x_{in} = 0. and x_{in} corresponding to the compensated trajectory

On the compensated trajectory the values of the synchrotron integrals I_2 and I_3 are:

$$I_2 = 1.38\ m^{-1} \qquad I_3 = 1.33\ m^{-2}$$

giving for the whole ring

$$I_2 = 10.01\ m^{-1}\ (9.76\ m^{-1})\ I_3 = 8.52\ m^{-2}\ (8.07\ m^{-2})$$

quite similar to those within brackets computed with the previous field model[5].

5. MULTIPOLAR ANALYSIS

The general scalar magnetic multipolar potential of order m in cylindrical coordinates can be written as[3]

$$P_m(r,\theta,z) = \frac{r^m \sin(m\theta)}{m!}\ G_m(r,z) \qquad 5.1)$$

where the condition of satisfying the Laplace equation is equivalent to:

$$\frac{\partial^2 G_m}{\partial r^2} + \frac{2m+1}{r}\ \frac{\partial G_m}{\partial r} + \frac{\partial^2 G_m}{\partial z^2} = 0 \qquad 5.2)$$

Writing the solution of 5.2) as

$$G_m(r,z) = \sum_{k=0}^{\infty} G_{m2k}(z)\ r^{2k} \qquad 5.3)$$

one can demonstrate that:

$$G_{m2k}(z) = (-1)^k\ \frac{m!}{4^k (m+k)!\ k!}\ \frac{\partial^{2k} G_{mo}}{\partial z^{2k}} \qquad 5.4)$$

If there is no dependence on z, the potential contains only the first term of the sum 5.3) for each multipole: for example a pure dipole is described in Cartesian coordinates with $r^2=x^2+y^2$ by:

$$P_1(x,y) = y\ G_{10} \qquad 5.5)$$

while if there is dependence on z, as for example in the wiggler, the dipole potential becomes:

$$P_1(x,y,z) = y\ [\ G_{10}(z) + G_{12}(z)\ r^2 + G_{14}(z)\ r^4 + \ldots\ ] \qquad 5.6)$$

The measured $B_y(0,0,z)$ coincides with $G_{10}(z)$.

We will try to fit the wiggler potential on the data with a dipole plus a sextupole term namely:

$$P(x,y,z) = P_1(x,y,z) + P_3(x,y,z) \qquad 5.7)$$

Using 5.1) and 5.3) and dropping of order higher than third we get:

$$P(x,y,z) = y\, G_{10}(z) + (x^2y + y^3)\, G_{12}(z) + \frac{3x^2y - y^3}{6}\, G_{30}(z) \qquad 5.8)$$

and hence:

$$B_x(x,y,z)= xy\, [2\, G_{12}(z) + G_{30}(z)] \qquad 5.9)$$

$$B_y(x,y,z)= G_{10}(z) + (x^2 + 3y^2)\, G_{12}(z) + \frac{x^2 - y^2}{2}\, G_{30}(z) \qquad 5.10)$$

$$B_z(x,y,z)= y\, \frac{\partial G_{10}}{\partial z} + (x^2y + y^3)\, \frac{\partial G_{12}}{\partial z} + \frac{3x^2y - y^3}{6}\, \frac{\partial G_{30}}{\partial z} \qquad 5.11)$$

From the condition on the Laplacian:

$$\Delta P=0 \qquad 5.12)$$

and by derivation with respect to each coordinate x_i (i = x,y,z) we get:

$$\Delta \frac{\partial P}{\partial x_i} = \Delta B_i = 0 \qquad 5.13)$$

Applying to the vertical component we deduce easily:

$$\frac{\partial^2 B_y}{\partial x^2} = 2\, G_{12}(z) + G_{30}(z) \qquad 5.14)$$

$$\frac{\partial^2 B_y}{\partial y^2} = 6\, G_{12}(z) - G_{30}(z) \qquad 5.15)$$

$$\frac{\partial^2 B_y}{\partial z^2} = \frac{\partial^2 G_{10}}{\partial z^2} = -\, 8\, G_{12}(z) \qquad 5.16)$$

ΔB_y can be made to vanish with any arbitrary $G_{10}(z)$ and $G_{30}(z)$.

The Laplacian computed with the three second derivatives of B_y derived from the field measurements (see paragraph 3) comes out to be different from zero: the data are not completely consistent. This is due with the limited range of vertical positions reachable by the probe, which considerably restricts the sensitivity of the second derivative measurement. We can partially face this inconvenient by taking into account only a consistent set of measurements. These are of course $B_y(0,0,z)$ and $B_y(x,0,z)$, from which one can deduce $\partial^2 B_y / \partial z^2$ and $\partial^2 B_y / \partial x^2$. From the previous formulae we get G_{12} and G_{30} (see Figs. 15 and 16).

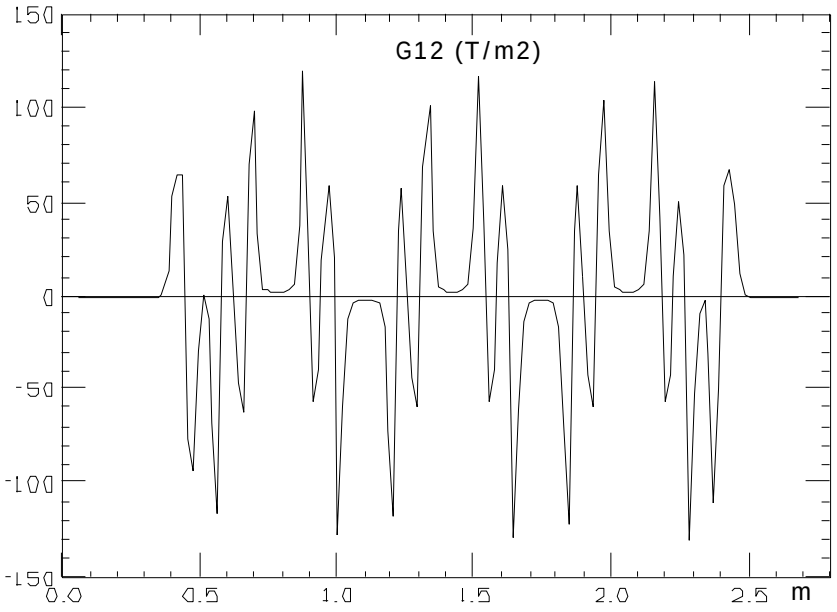

Fig. 15 - Function $G_{12}(z)$

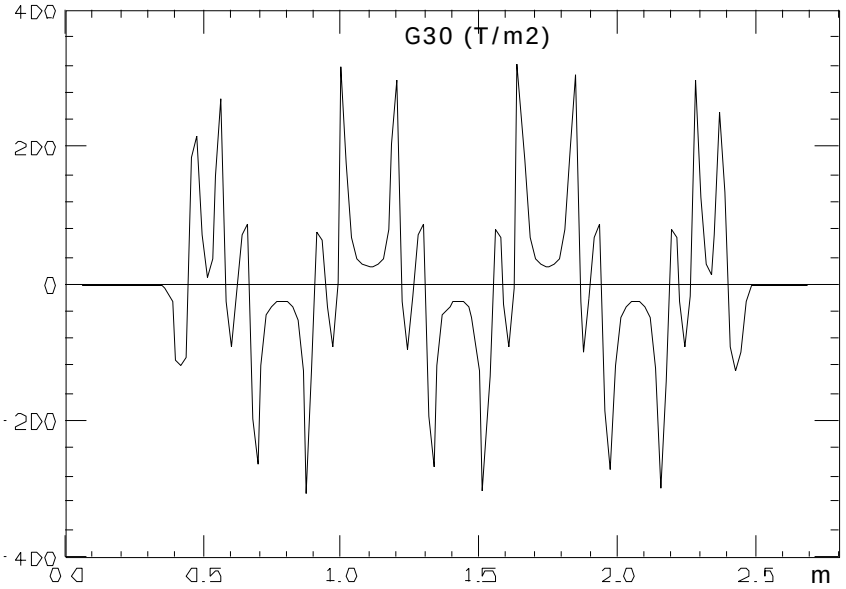

Fig. 16 - Function $G_{30}(z)$

The $G_{30}(z)$ term corresponds to a normal sextupole component. It is present also on pole centers, while the pseudo sextupole $G_{12}(z)$ arises only on the fringing regions. The integrals of the two components over the whole wiggler are:

$$\int_0^{z_F} G_{30}(z)\, dz = -2.3 \text{ T/m} \qquad 5.20)$$

$$\int_0^{z_F} G_{12}(z)\, dz = -4.0 \times 10^{-5} \text{ T/m} \qquad 5.21)$$

i.e, the total integral of the pseudo sextupole G_{12} is zero, while there exist a net component of the 'normal' sextupolar field, in good agreement with the value estimated in [1].

Using 5.9), 5.10) 5.14) and 5.15) we can write the quadratic components of the field as:

$$B_x = \frac{\partial^2 B_y}{\partial x^2}\, xy \qquad 5.22)$$

$$B_y = \frac{\partial^2 B_y}{\partial x^2}\, \frac{x^2}{2} + \frac{\partial^2 B_y}{\partial y^2}\, \frac{y^2}{2} \qquad 5.23)$$

which in terms of the functions defined in paragraph 3 become:

$$B_x = 2\, a_2(z)\, xy \qquad 5.24)$$

$$B_y = a_2(z)\, x^2 + b_2(z)\, y^2 \qquad 5.25)$$

The function $b_2(z)$ can be obtained from formula 5.15) using the same set of data (1÷6) used for the computation of $a_2(z)$. The integrals of the two functions on each pole are:

Table III - Integral of sextupolar components on Wiggler poles

POLE NUMBER	$\int a_2(z)\, dz$ (T/m)	$\int b_2(z)\, dz$ (T/m)
1	4.1	-13.2
2	-11.1	26.2
3	11.2	-26.5
4	-11.0	26.3
5	11.1	-26.2
6	-11.2	25.4
7	4.5	-10.9
Total integral	-2.3	1.1

For tracking purposes the function $a_2(z)$ can be approximated on each full pole by two thin lenses with an integrated strength of ± 5.5 T/m (with alternating signs), centered on the maximum of the function, occurring at ~10 cm from the pole center. In the two end poles the same approximation is made with two lenses positioned at 5.5 cm from the pole center and with integrated strength of 2.17 T/m. The algebraic sum of the strengths is equal to the total integral (-2.3 T/m). It is worth recalling that the value of the horizontal coordinate x must be corrected with the offset of the central orbit, which in the position of lenses corresponds to ±7 mm with respect to the wiggler axis.

The function $b_2(z)$ has four peaks on each pole: the two on the side are compensated by those of the adjacent pole and can be neglected. The two higher peaks, centered on the same position of the $a_2(z)$ peaks, can be represented by thin lenses with integrated strength ± 12.5 T/m. The two end poles can be represented by a one lens of 13 T/m centered on the pole end, and two lenses of -12.5 T/m, centered also in the same position of those of $a_2(z)$.

6. LIMIT FOR B_x ---> 0

We can observe that, on the average, $\partial^2 B_y/\partial x^2$ is very small with respect to the other two second derivatives. This can be explained by observing that the wiggler gap has an horizontal size much larger than the vertical one. Let us assume therefore the limiting case, where the field does not depend on x at all. We assume furthermore that the potential has contributions from dipole, sextupole and decapole:

$$P(x,y,z) = y\, G_{10}(z) + (x^2y + y^3)\, G_{12}(z) + (x^4y + 2x^2y^3 + y^5)\, G_{14}(z) +$$

$$+ \frac{3x^2y - y^3}{6}\, G_{30}(z) + \frac{3x^4y + 2x^2y^3 - y^5}{6}\, G_{32}(z) + \qquad 6.1)$$

$$+ \frac{5x^4y - 10x^2y^3 + y^5}{120}\, G_{50}(z)$$

From 5.4) we get:

$$G_{12} = -\frac{1}{8}\frac{\partial^2 G_{10}}{\partial z^2} \qquad 6.2)$$

$$G_{14} = \frac{1}{192}\frac{\partial^4 G_{10}}{\partial z^4} \qquad 6.3)$$

$$G_{32} = -\frac{1}{16}\frac{\partial^2 G_{30}}{\partial z^2} \qquad 6.4)$$

The coefficient of the x^2y term in 6.1) vanishes if:

$$G_{30} = -\,2\,G_{12} = \frac{1}{4}\frac{\partial^2 G_{10}}{\partial z^2} \qquad 6.5)$$

and therefore:

$$G_{32} = -\frac{1}{64}\frac{\partial^4 G_{10}}{\partial z^4} \qquad 6.6)$$

Similarly the coefficient of x^4y is zero if:

$$G_{50} = \frac{1}{16}\frac{\partial^4 G_{10}}{\partial z^4} \qquad 6.7)$$

The potential can then be written as a function of G_{10} only:

$$P(x,y,z) = y\,G_{10}(z) + \frac{\partial^2 G_{10}}{\partial z^2}\left(\frac{x^2\,y + y^3}{8} + \frac{3x^2y - y^3}{24}\right) +$$

$$+ \frac{\partial^4 G_{10}}{\partial z^4}\left(\frac{x^4y + 2x^2y^3 + y^5}{192} - \frac{3x^4y + 2x^2y^3 - y^5}{384} + \frac{5x^4y - 10x^2y^3 + y^5}{1920}\right) \qquad 6.8)$$

where we can verify that any the dependence on x disappears:

$$P(y,z) = y\,G_{10}(z) - \frac{y^3}{6}\frac{\partial^2 G_{10}}{\partial z^2} + \frac{y^5}{120}\frac{\partial^4 G_{10}}{\partial z^4} \qquad 6.9)$$

B_y and B_z must satisfy Maxwell equations in the (y,z) plane. From the expression above we obtain:

$$B_y(y,z) = G_{10}(z) - \frac{y^2}{2}\frac{\partial^2 G_{10}}{\partial z^2} + \frac{y^4}{24}\frac{\partial^4 G_{10}}{\partial z^4} \qquad 6.10)$$

$$B_z(y,z) = y\frac{\partial G_{10}}{\partial z} - \frac{y^3}{6}\frac{\partial^3 G_{10}}{\partial z^3} + \frac{y^5}{120}\frac{\partial^5 G_{10}}{\partial z^5} \qquad 6.11)$$

If we try to verify that div(B)=0 and curl(B)=0 we get:

$$\frac{\partial B_y}{\partial y} + \frac{\partial B_z}{\partial z} = \frac{y^5}{120}\frac{\partial^5 G_{10}}{\partial z^5} \qquad 6.12)$$

$$\frac{\partial B_y}{\partial z} - \frac{\partial B_z}{\partial y} = \frac{\partial G_{10}}{\partial z} - \frac{y^2}{2}\frac{\partial^3 G_{10}}{\partial z^3} + \frac{y^4}{24}\frac{\partial^5 G_{10}}{\partial z^5} - \frac{\partial G_{10}}{\partial z} +$$

$$+ \frac{y^2}{2}\frac{\partial^3 G_{10}}{\partial z^3} - \frac{y^4}{24}\frac{\partial^5 G_{10}}{\partial z^5} = 0 \qquad 6.\ 13)$$

Therefore Maxwell equations are satisfied up to the fifth order. Clearly, more high order multipoles are taken into account, more precisely the deviations are defined.

It is amusing to verify that by choosing $G_{10}(z) = kz$, we get a quadrupole

$$B_y(y,z) = kz \qquad B_z(y,z) = ky \qquad 6.14)$$

if $G_{10}(z)=kz^2$ we get a sextupole

$$B_y(y,z) = k(z^2 - y^2) \qquad B_z(y,z) = 2\,k\,yz \qquad 6.15)$$

and with $G_{10}(z) = kz^3$ an octupole

$$B_y(y,z) = k(z^3 - 3\,y^2z) \qquad B_z(y,z) = k(3\,yz^2 - y^3) \qquad 6.16)$$

and so on.

REFERENCES

[1] B. Bolli, F. Iungo, M. Modena, M. Preger, C. Sanelli, F. Sgamma, S. Vescovi: "Measurements on the Wiggler Magnet for the DAΦNE Main Rings", DAΦNE TECHNICAL NOTE M-4, April 1994.

[2] R.H. Helm, M.J. Lee, P.L. Morton, M. Sands: "Evaluation of synchrotron radiation integrals", IEEE Trans. Nucl. Sci. NS-20 (1973).

[3] M. Bassetti: "Analytical formulae for multipole potentials", DAΦNE Technical Note G-26, July 1994.

[4] NAG Foundation Library Handbook.

[5] M.E. Biagini, S. Guiducci, M.R. Masullo, G. Vignola: "DAΦNE Lattice Update'", DAΦNE Technical Note L-4, December 1991.